Supplementary Information

for

Construction of a Dual Z-Scheme g-C_3N_4/BiOI/Ag_2CrO_4 Ternary Heterojunction for Highly Efficient Visible-Light Photocatalytic Degradation of Sudan Red III

Xianfeng Zhang,* Hao Zhang, Jingbo Lu, Sun Zhao, Jianjian Cheng, Han Zhou, Yuting Liang

Anhui Provincial Engineering Research Center of Silicon-Based Materials, School of Material and Chemical Engineering, Bengbu University, Bengbu, 233030, P. R. China

*Corresponding author

E-mail: zxf@bbc.edu.cn

S1. Characterization

X-ray diffraction (XRD) analysis was conducted on a Rigaku SmartLab SE diffractometer (Japan) with copper target operated at 40 kV and 50 mA to determine the crystal structure and phase composition. Diffraction patterns were recorded over a 2θ range of 10° to 80° with a scanning speed of 20° min^{-1}. Fourier-transform infrared spectroscopy (FTIR) spectra were acquired using a Thermo Fisher Scientific Nicolet iS10 spectrometer (USA). Samples were prepared as pellets with KBr. Spectral data were collected in the wavenumber range of 4000 to 400 cm^{-1}. The surface morphology and microstructure of the samples were examined using field-emission scanning electron microscopy (FE-SEM) on a Hitachi S4800 instrument (Japan). Transmission electron microscope (TEM) images were obtained using JEOL JEM-F200 at 200 kV (Japan). X-ray photoelectron spectroscopy (XPS) was employed for surface elemental analysis and chemical state identification. Measurements were carried out on a Thermo Fisher Scientific ESCALAB 250Xi spectrometer (USA). N_2 adsorption–desorption isotherms were recorded on a Micromeritics TriStar II 3020 analyzer (USA). Prior to measurement, the sample was degassed at 473 K for 5 h. The specific surface area was calculated using the Brunauer–Emmett–Teller (BET) method, and the pore-size distribution was derived from the desorption branch using the Barrett–Joyner–Halenda (BJH) model. Photoluminescence spectra were recorded on a Hitachi F4600 fluorescence spectrometer. UV-Vis diffuse reflectance spectroscopy (DRS) were examined using a Hitachi U-3900 spectrophotometer (Japan). The scanning range was 200–800 nm. The absorbance of Sudan Red III solution (λmax = 509 nm) was measured at given time intervals. The metal leaching concentration during the photocatalytic process was tested using an Agilent 7800 inductively coupled plasma mass spectrometer (ICP-MS) from the United States. Electron spin resonance (ESR) spectra were acquired on a Bruker EMXplus-6 spectrometer (Germany) using 5,5-dimethyl-1-pyrrolidine N-oxide (DMPO) as the spin-trapping probe. The photoelectric performance signal test was completed on CHI760E (China).

S2. Calculation of apparent quantum yield (AQY)

$$AQY = \frac{\upsilon \times N_A \times K}{\frac{I \times A \times \lambda \times t}{h \times c}} = 0.0012\%$$

υ: The reaction rate (mol·s^{-1}) is usually taken as the initial linear stage reaction rate.Based on the initial concentration of Sudan III C_0 (40 mg·L^{-1}), the reaction rate value can be calculated as 3.595×10^{-9} mol·s^{-1} from the absorbance change in the first 10 minutes of photocatalysis and the molecular weight of Sudan III (352.39 g·mol^{-1}).
K: The number of electrons transferred in the reaction is determined by the target product. The ring opening cleavage of azo bonds in Sudan III is the first step in decolorization, bleaching, and subsequent degradation, with an electron transfer number of 4, so K=4.
I: Optical power density (370 W·m^{-2}).

A: Incident illumination area (1.59×10^{-3} m^2).

λ: The wavelength of the incident monochromatic light (420 nm).
t: Reaction time (600 s).

h: Planck constant (6.62×10^{-34} J·s).

c: The speed of light (3.0×10^{8} m·s^{-1}).

N_A: Avogadro constant (6.02×10^{23} mol^{-1}).

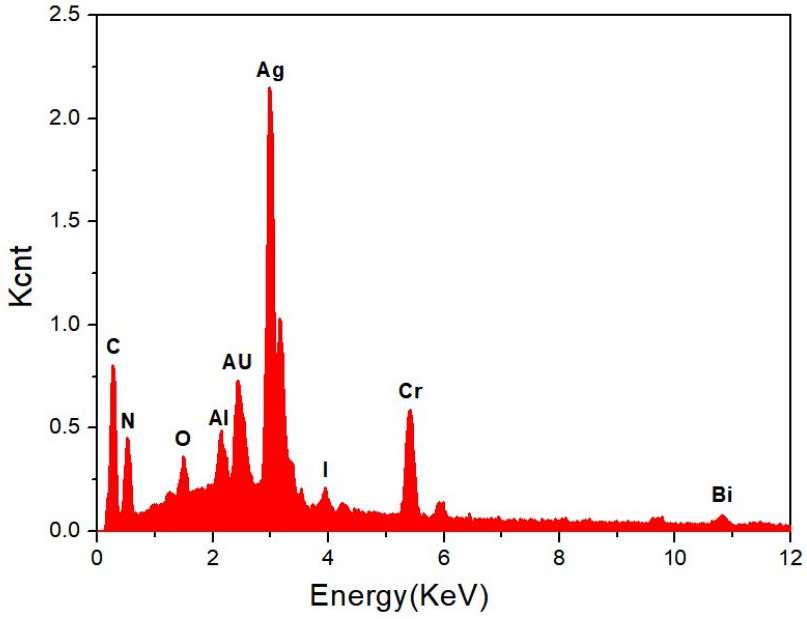

Fig. S1 EDX energy spectrum of the 30%-g-C_3N_4/BiOI/Ag_2CrO_4 composite.

Table S1 Mass percentage and atomic percentage of 30%-g-C_3N_4/BiOI/Ag_2CrO_4 in EDS analysis.

Element	Wt%	At%
C K	21.02	54.12
N K	01.60	03.54
O K	11.68	22.58
BiM	12.82	01.90
AgL	40.10	11.49
I L	03.46	00.84
CrK	09.31	05.54

Table S2 Summary of the pore structural parameters for different samples.

Catalyst	S_{BET} /(m^2/g)	Pore volume /(cm^3/g)	Pore size /(nm)
g-C_3N_4	5	0.01	9.5
g-C_3N_4/BiOI	23	0.05	8.7
30%-g-C_3N_4/BiOI/Ag_2CrO_4	13	0.03	10.6

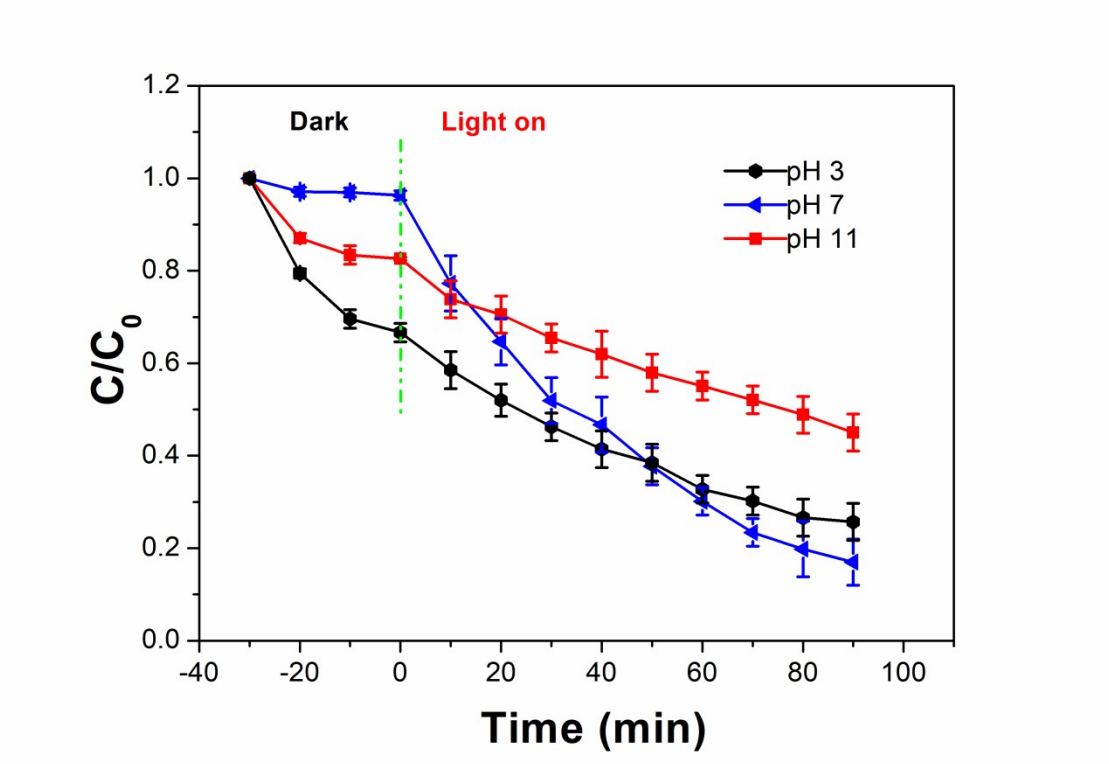

Fig. S2 Effect of pH plot using the 30%-g-C_3N_4/BiOI/Ag_2CrO_4 nanocomposite.

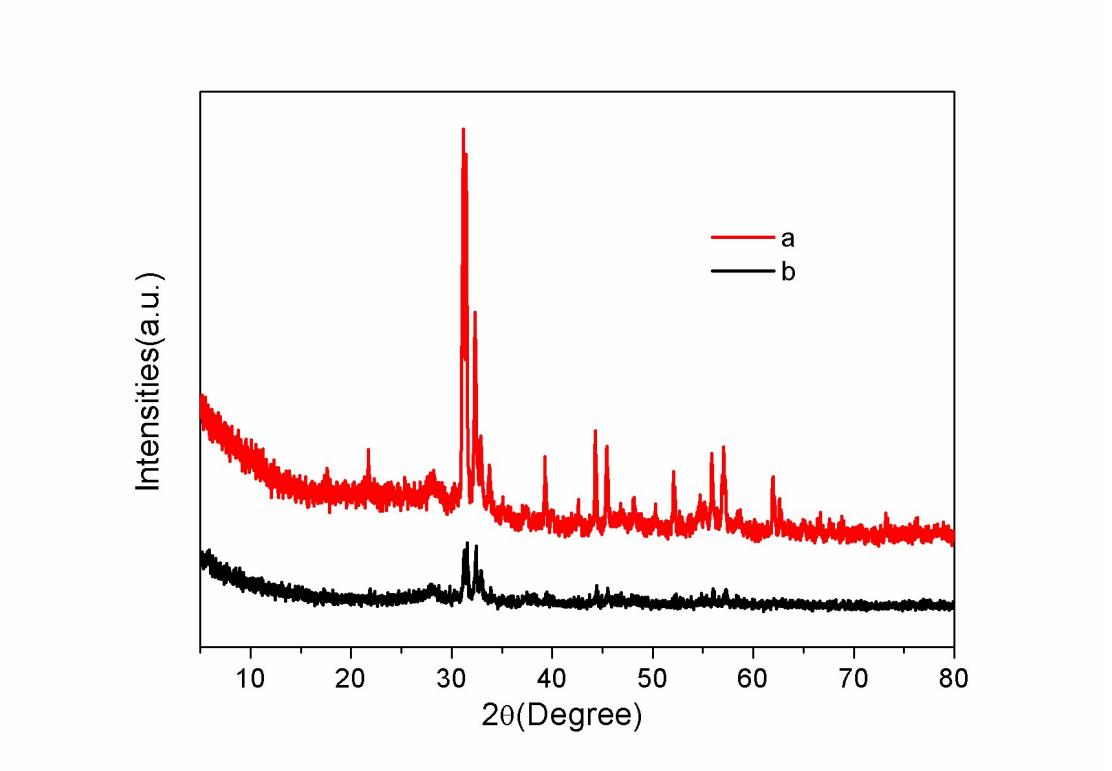

Fig. S3 XRD of 30%-g-C_3N_4/BiOI/Ag_2CrO_4 composite before (a) and after (b) photocatalytic reaction.

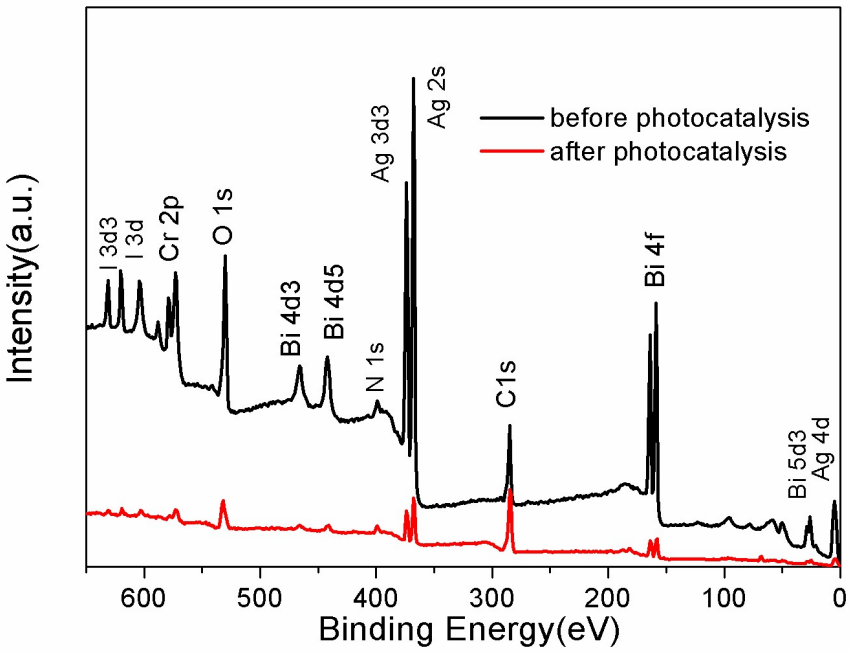

Fig. S4 XPS of 30%-g-C_3N_4/BiOI/Ag_2CrO_4 composite before and after photocatalytic reaction.

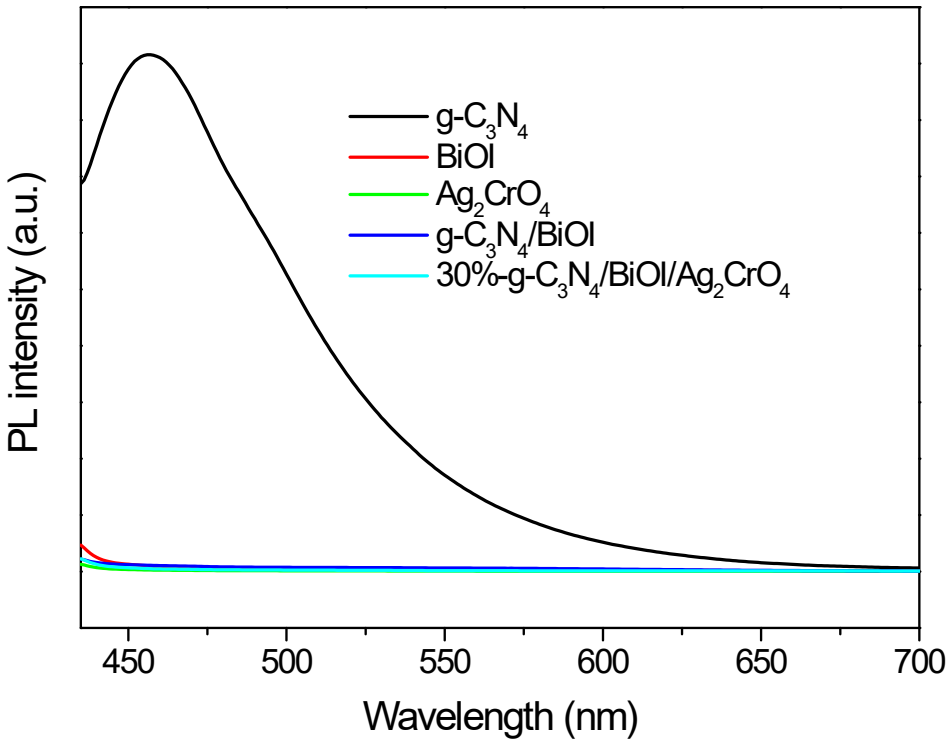

Fig. S5 Photoluminescence spectra of g-C_3N_4, BiOI, Ag_2CrO_4, g-C_3N_4/BiOI and the 30%-g-C_3N_4/BiOI/Ag_2CrO_4 composite irradiated at 420 nm.

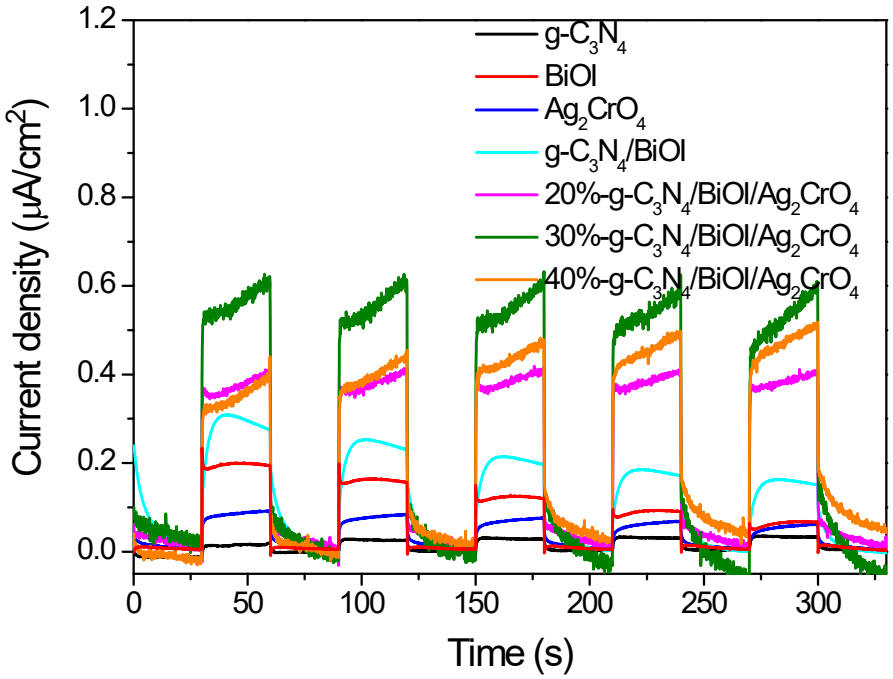

Fig. S6 The transient photocurrent response of the as-synthesized catalysts.